GRADIENT PATTERN ANALYSIS APPLIED FOR COMPUTER VISION IN MEDICAL ULTRASOUND DIAGNOSIS

Rubens Andreas Sautter[1], Reinaldo Roberto Rosa[1], Debora Cristina Alavarce[2] and Daniel Guimarães Silva[2]

[1]Applied Computing Program (CAP), National Institute for Space Research (INPE)
Av. dos Astronautas, 1.758, CEP 12245-027, São José dos Campos/SP - Brazil
[2]Hipocampus EdTech - Digital Learning
R. do Serimbura, 320, CEP 12243-360, São José dos Campos/SP - Brazil

ABSTRACT

This paper describes a new application of the technique known as Gradient Pattern Analysis (GPA), focused here on computer vision. In the GPA domain, the image is translated into a tessellation triangulation field based on the vectors positions that make up the gradient lattice of the matrix image. The GPA version considered here generates three attributes (G1, G2 and G3) that can be used as labels for a supervised machine-learning model. The case study presented here shows that GPA is a useful tool for real-time fetal biometry from 2D ultrasound images. The application in obstetrics indicates that the technique can also be useful for learning diagnostic imaging in gynecology, hepatology and oncology. The generalization of the technique to other applications in practical learning in health is discussed.

KEYWORDS

Gradient Pattern Analysis, Computer Vision, Supervised Machine Learning, 2D Endoscopic Ultrasound Biometry

1. INTRODUCTION

Gradient Pattern Analysis (GPA) is a technique for analyzing the dynamics of nonlinear 2D-spatiotemporal systems, which is based on the gradient symmetry-breaking properties of a matrix snapshot sequence. Originally, GPA has found numerous applications in 2D dynamic systems [Rosa et al., 1999, da Silva et al., 2000, Faria et al., 2007; Baroni et al., 2006, Freitas et al., 2010]. GPA was originally inspired by 2D turbulence analysis in space (Andrade et al., 2006) and environmental physics (Velho et al. 2001). In the last five years, the technique has been improved for automatic morphological classification associated with supervised training of machine learning models, especially with hybrid Deep Learning (CNN combined with RNN). In the scope of computer vision, GPA "sees" different morphologies in both the gradient field and the correspondent triangulation domains from where a set of metrics are extracted as in the application in galaxy morphology (Barchi et al., 2019, Rosa et al, 2018). The gradient field metrics (the so-called “gradient moments”) are extracted based on the geometry of the gradient field (via Delaunay triangulation) and also on the norm and phase matrices of the correspondent gradient field. GPA is therefore a set of computational operations on a given numerical lattice (as a matrix) and on the gradient pattern of a digital image.

In the field of medical images, diagnostic ultrasounds offer information about internal areas and parts of the body, such as the liver, kidneys health, and reproductive organs. The main application explored here examines an unborn baby and checks its health and growth status. Therefore, identifying the baby (especially the head and face) by 2D ultrasound is a detection task that will be used here as a case study to test the feasibility and usefulness of GPA in diagnostic medical imaging.

2. DATA, METHODOLOGY AND RESULTS

Our approach uses ultrasound recordings provided by the Projeto FAPESP database (process No 2021/15114-8) in partnership with the Brazilian company Hipocampus EdTech. The basic example consists of a set of 2 movies composed by 542 snapshots each, recorded in gray scale, for an 18 and 15-week-old baby.

The GPA as an analytical method explores a new paradigm proposing to analyze, instead of the absolute values of the matrix amplitudes, the symmetry breaking in the gradient field of a given matrix. The symmetry to be broken, considered in the original version of the technique (Rosa, Sharma, Valdivia, 1999; Rosa et al., 2018), are the bilateral symmetries in relation to the vertical and horizontal axes. In the first operation of GPA, the Matrix Gradient Lattice is computed in the x-direction and the y-direction, whenever possible, with Central Finite Difference. The boundaries are measured with forward and backward finite differences. The gradient lattice (GL) of a matrix is composed of V vectors of which a portion V_A is asymmetric (bilaterally symmetric pairs in the gradient lattice are those that, for a given tolerance, have the same module and opposite phases). After obtaining the GL from a matrix, the first three gradient moments are calculated as follows:

$$G_1 = \frac{T_A - V_A}{V_A} \tag{1}$$

where T_A is the number of edges that represent the connection between the V_A asymmetric vectors obtained from the Delaunay triangulation performed on the GL. The measure, G_2, based on the norms of *each asymmetric vector* v_i, is de defined as:

$$G_2 = \frac{V_A}{V}\left(1 - \frac{\left|\sum_{i=0}^{V_A} v_i\right|}{2\sum_{i=0}^{V_A}|v_i|}\right) \tag{2}$$

Note that if all vectors are symmetrical, G_2 = 0.0. The measure, G_3, based on the phase of *each asymmetric vector* v_i, depends on the vector phases (φ) and the angle of each vector with respect to the symmetry center (θ) of the matrix, and is defined as:

$$G_3 = \frac{1}{2}\left(\frac{V_A}{V} + \frac{1}{2V_A}\sum_{i=0}^{V_A}(u_i.v_i + 1)\right) \tag{3}$$

Note that, the dot product is maximum ($u.v$ = 1) when the position of the vector is aligned with its phase, zero when they are perpendicular, and minimum ($u.v$ = −1) when they are opposite.

Figure 1 shows the application of preprocessing GPA on a snapshot of the one of the ultrasound videos analyzed in this work. In order to enable visualization of the corresponding gradient lattice, the original image is reduced (to 32x32) in order to intensify the typical bilateral asymmetry of the baby's head contour (image (b) immersed in the original image (a)). The corresponding gradient lattice is shown in Figure 1c. The yellow grid with vertical and horizontal axes identifies the references for bilateral symmetry breaking. The tip of the baby's nose, for example, imposes a strong break in symmetry between the fourth and second quadrants. For the calculation of G_1 the triangulation between the vectors is performed. As shown in Figure 2, the triangulation is also useful to highlight fluctuations in norms and phases throughout the dynamics whose main objective is to identify the baby in the video.

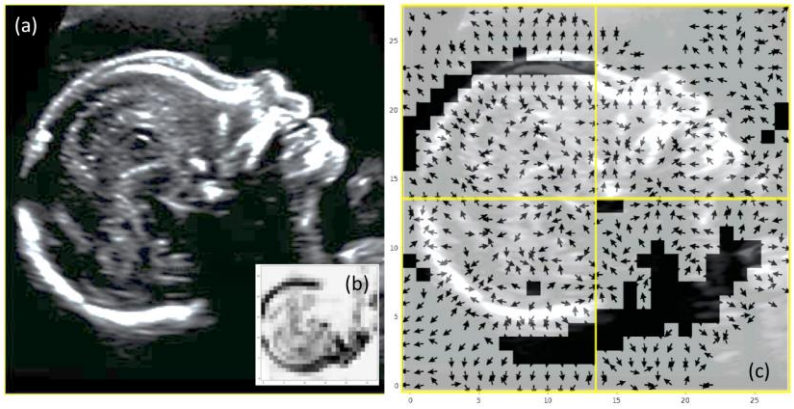

Figure 1. (a) The original image (a snapshot from the ultrasound video); (b) the reduced image and (c) the superposed correspondent gradient lattice with the bilateral symmetry axis

In our approach GPA is applied to each snapshot within a dashboard context. As shown in Figure 2, the measures G_1, G_2 and G_3 work as monitoring scores and are shown on a dashboard developed in Python (dash library). Figure 2 shows the application of the dashboard on the complete ultrasound, in a monitored way, and indicates the moment (peak) in the G_3 metric (of the phases) when the head (with details of the face and arm) are detected with great emphasis. The dashboard shows the original snapshot (left), the same with triangulation (middle) and the histogram of all phases of the vectors that make up the gradient field.

Figure 2 shows the application of the dashboard on the complete ultrasound, in a monitored way, and indicates the moment (peak) in the G_3 metric (of the phases) when the head (with details of the face and arm) are detected with great emphasis. The dashboard shows the original snapshot (left), the same with triangulation (middle) and the histogram of all phases of the vectors that make up the gradient field.

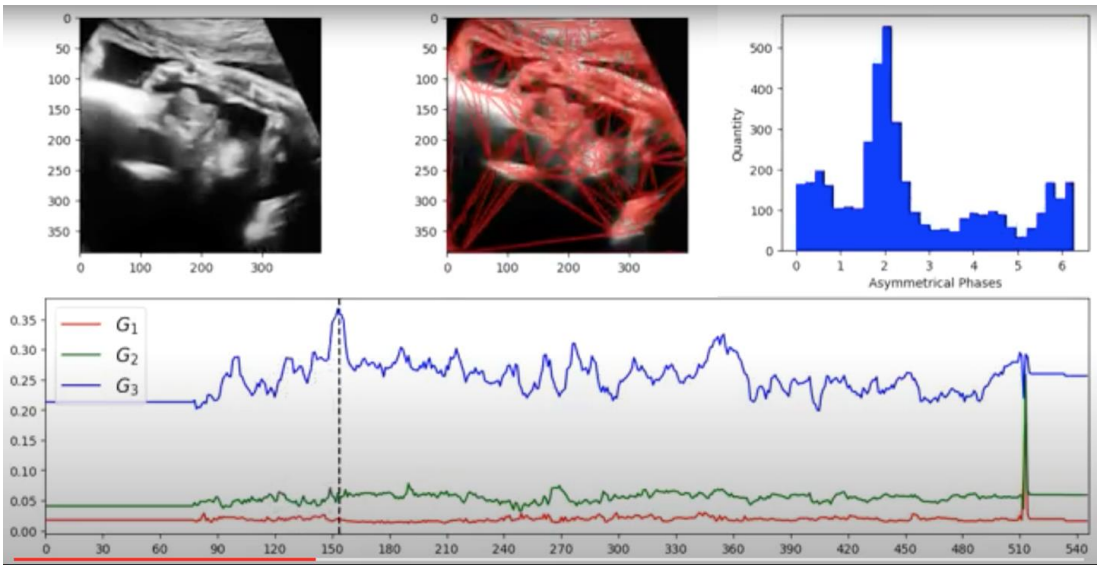

Figure 2. The GPA dashboard for the Ultrasound Diagnosis. The high performance of G_3 is remarkable even when the arm of the baby is in scene. The histogram of the phases of the asymmetric vectors works as a less accurate indicator of target detection

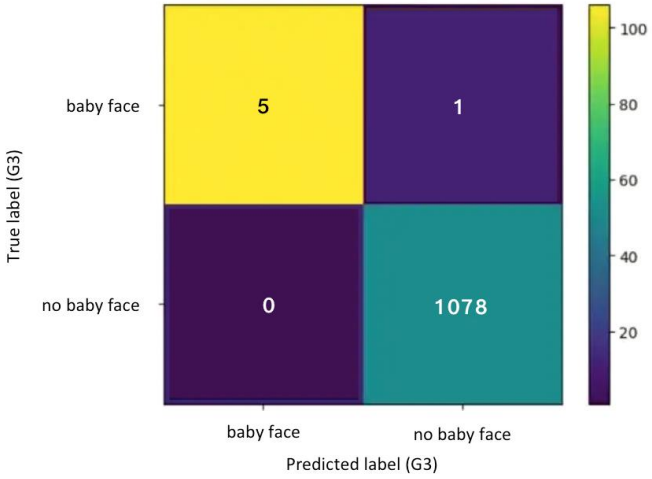

Figure 3. Confusion Matrix based on G_3 as a label

The total sample has 1084 snapshots. Of this total, the sought pattern (baby face) was identified 3 times in each one, totaling 6 positive identifications. The G_3 label was within the range from 0.27 to 0.38 for 5 identifications and only one identification was outside of this range (G_3=0.21) for a snapshot that was also visually validated. Based on this sample, a confusion matrix prototype was created (Figure 3) with these values to guide the exploration of supervised training based on GPA (G_3).

3. CONCLUSION

The preliminary analysis applied to the chosen case study makes it clear that the GPA-G_3 metric is adequate to capture the morphological information sought in ultrasound imaging diagnosis (especially when applied in real time). In two applications having 6 positive patterns in a sample of 1084 snapshots, the expected positive result was 83% (5/6). This result indicates the G_3 metric as the most suitable to be used as a label for supervised training of a hybrid deep learning model that is under development (using CNN with LSTM).

It is noteworthy that the methodology presented here can be useful in diagnosis by medical imaging in other paradigms of health sciences, emphasizing that it can also be effective in the training and learning process in identifying patterns in ultrasound exams and other techniques that require training to detect patterns in endoscopic medical footage or equivalent applications in other fields of computer vision. More recently, testing of new computer vision techniques for diagnostics based on AI is encouraged within the space medicine program under the ISI and Artemis mission (Krittanawong et al. 2023).

ACKNOWLEDGEMENT

The authors would like to thank FAPESP for financial support via Project Nº 2021/15114-8.

REFERENCES

Andrade, A.P., Ribeiro, A.L.B., Rosa, R.R., 2006. Gradient pattern analysis of cosmic structure formation: Norm and phase statistics, Physica D, Vol. 223(2), pp. 139-145. DOI: 10.1016/j.physd.2006.08.025.

Barchi, P.H. et al, 2020. Machine and Deep Learning applied to galaxy morphology - A comparative study, *Astronomy and Computing*, Vol. 30, No. 1, pp. 100334. DOI: 10.1016/j.ascom.2019.100334.

Baroni, M.P.M.A. et al, 2006. Modeling and gradient pattern analysis of irregular SFM structures of porous silicon, *Microelectronics Journal*, Vol. 37, No. 4, pp. 290-294. DOI: 10.1016/j.mejo.2005.05.029.

Costa-Junior, R.A. et al, 2005. Gradient pattern analysis of extended convection-diffusion, *Physica A: Statistical Mechanics and its Applications*, Vol. 344, No. 3-4, pp. 447-455. DOI: 10.1016/j.physa.2004.06.013.

da Silva, F.A., Rosa, R.R., Roman, L.S., Veje, E., Pepe, I., 2000. Characterization of asymmetric fragmentation patterns in SFM images of porous silicon, *Solid State Communications*, Vol. 113(12), pp. 703-708. DOI: 10.1016/S0038-1098(99)00557-8.

de Freitas, R.M. et al, 2010. Using Gradient Pattern Analysis for land use and land cover change detection, *IEEE International Geoscience and Remote Sensing Symposium*, Honolulu, Hawaii, pp. 3648-3651. DOI: 10.1109/igarss.2010.5650698.

Faria, L.N. et al, 2007. A parallel application for 3D reconstruction of coronal loops using image morphing, *Image and Vision Computing*, Vol. 25, No. 1, pp. 95-102. DOI: 10.1016/j.imavis.2005.12.007.

Krittanawong, C. et al. 2023. Human Health during Space Travel: State-of-the-Art Review, Cells, Vol. 12, pp. 12-32, DOI: 10.3390/cells12010040.

Rosa, R.R. et al, 1999. Characterization of asymmetric fragmentation patterns in spatially extended systems, *International Journal of Modern Physics C*, Vol. 10, No. 1, pp. 147-163. DOI: 10.1142/S0129183199000103.

Rosa, R.R. et al, 2000. Gradient pattern analysis of Swift-Hohenberg dynamics: phase disorder characterization, *Physica A: Statistical Mechanics and its Applications*, Vol. 283, No. 1-2, pp. 156-159. DOI: 10.1016/S0378-4371(00)00144-8.

Rosa; R.R., et al, 2018. Gradient pattern analysis applied to galaxy morphology, *Monthly Notices of the Royal Astronomical Society: Letters*, Vol. 477, No. 1, pp. L101—L105. DOI: 10.1093/mnrasl/sy054

Velho, H.F.C. et al., 2001. Multifractal model for eddy diffusivity and counter-gradient term in atmospheric turbulence, Physica A, 295 (1-2), pp. 219-223. DOI: 10.1016/S0378-4371(01)00077-2.

Veronese, T.B. and Martins, M.P.A., 2010. Biologically Motivated Fuzzy-like Measure for Complex Structures Perception, *Journal of Computational Interdisciplinary Sciences*, Vol. 1, No. 3, pp. 233-239. DOI: 10.6062/jcis.2010.01.03.0025.